Electronic Supplementary Material (ESI) for Inorganic Chemistry Frontiers.

Electronic Supplementary Information

Enhancing Interfacial Charge Transfer in Mesoporous MoS_2/CdS Nanojunction Architectures for Highly Efficient Visible-Light Photocatalytic Water Splitting

Chrysanthi Patriarchea,[a] Ioannis Vamvasakis,[a] Eirini D. Koutsouroubi,[a] Gerasimos S. Armatas*[a]

[a] Department of Materials Science and Technology, University of Crete, Heraklion 70013, Greece. E-mail: garmatas@materials.uoc.gr

Table S1. Comparison of H_2-production activities for different reported MoS_2/CdS-based photocatalysts.

Photocatalyst	Reaction Conditions	Light Source	H_2 evolution rate		Quantum Efficiency (QE)	Ref.
			($\mu mol\ h^{-1}$)	($\mu mol\ g^{-1}\ h^{-1}$)		
0.2 wt.% MoS_2/CdS	100 mg catalyst, 10 % v/v lactic acid	300 W Xe lamp (λ≥420 nm)	540	5400	-	[1]
0.2 wt.% MoS_2 /CdS	100 mg catalyst, 10 % v/v lactic acid	300 W Xe lamp (λ≥420 nm)	533	5330	7.3% at 420 nm	[2]
0.9 mol% MoS_2/ CdS NPs	100 mg catalyst, 10 % v/v lactic acid	300 W Xe lamp (λ>420 nm)	1315	13150	-	[3]
6.9 wt.% feather-shaped MoS_2/CdS	50 mg catalyst, 0.5 M Na_2S, 0.5 M Na_2SO_3	300 W Xe lamp (λ≥400 nm)	192	3840	-	[4]
20 wt.% MoS_2 NSs/CdS NPs	20 mg catalyst, 10 % v/v lactic acid	300 W Xe lamp (λ≥400 nm)	137	6850	10.5% at 450 nm	[5]
15 wt.% MoS_2 /CdS NPs	80 mg catalyst, 0.1 M Na_2S, 0.02 M Na_2SO_3	300 W Xe lamp (λ≥400 nm)	382	4770	-	[6]
2 wt.% monolayer MoS_2/CdS	200 mg catalyst, 0.35 M Na_2S, 0.35 M Na_2SO_3	300 W Xe lamp (λ≥400 nm)	2100	10500	30.2% at 420 nm	[7]
	200 mg catalyst, 10 % v/v lactic acid		2590	12950	38.4% at 420 nm	
2 wt.% MoS_2/CdS microspheres	100 mg catalyst, 10 % v/v lactic acid	300 W Xe lamp (λ>400 nm)	406	4060	-	[8]
2.5 wt.% MoS_2 flowerlike/CdS nanorods	50 mg catalyst, 10 % v/v lactic acid	300 W Xe lamp (λ>400 nm)	551	11026	31.8% at 420 nm	[9]
20 wt.% 2D MoS_2/0D CdS	50 mg catalyst, 20 % v/v lactic acid	300 W Xe lamp (λ>400 nm)	84.8	1696	23.0% at 420 nm	[10]
10 wt.% MoS_2 NSs/CdS nanowires	20 mg catalyst, 20 % v/v lactic acid	300 W Xe lamp (λ≥400 nm)	1914	95700	46.9% at 420 nm	[11]
MoS_2/CdS NPs	60 mg catalyst, 10 % v/v lactic acid	300 W Xe lamp (λ≥420 nm)	314	5240	1.0% at 420 nm	[12]
10 wt.% MoS_2 NSs/CdS nanorods	200 mg catalyst, 10 % v/v lactic acid	300 W Xe lamp (λ≥420 nm)	9960	49800	41.4% at 420 nm	[13]
6.0 wt.% MoS_2 NSs/CdS nanorods	10 mg catalyst, 20 % v/v lactic acid	Natural solar irradiation	174	174000	-	[14]
1.0 wt.% MoS_2/CdS NSs	50 mg catalyst, 0.5 M Na_2S, 0.5 M Na_2SO_3	300 W Xe lamp (λ>400 nm)	87	1740	-	[15]
	50 mg catalyst, 20 % v/v lactic acid		436	8720		
MoS_2/CdS	20 mg catalyst, 25	300 W Xe lamp	775	38750	14.7%	[16]

nanomaterials (molar ratio of Mo:Cd=1:6)	% v/v lactic acid	(λ≥420 nm)			at 420 nm	
2 wt.% monolayer MoS_2/CdS	200 mg catalyst, 30 % v/v lactic acid, NaOH (pH~5)	300 W Xe lamp (λ≥420 nm)	1020	5100	-	[17]
CdS@MoS_2-5% irregular nanospheres	50 mg catalyst, 0.25 M Na_2S, 0.35 M Na_2SO_3	300 W Xe lamp (λ≥420 nm)	860	17203	24.2% at 420 nm	[18]
6.39 wt.% MoS_2/CdS NSs	100 mg catalyst, 0.35 M Na_2S, 0.25 M Na_2SO_3	300 W Xe lamp (λ≥420 nm)	3.7	370	0.65% at 420 nm	[19]
5 wt.% MoS_2 NSs/CdS particles	80 mg catalyst, 0.45 M Na_2S, 0.55 M Na_2SO_3	300 W Xe lamp (λ≥420 nm)	372	4650	7.3% at 420 nm	[20]
3 wt.% MoS_2/CdS hybrids	100 mg catalyst, 0.35 M Na_2S, 0.25 M Na_2SO_3	300 W Xe lamp (λ≥420 nm)	114	11400	1.2% at 420 nm	[21]
0.25 wt.% MoS_2 QDs/CdS	50 mg catalyst, 10 % v/v lactic acid	300 W Xe lamp (λ≥420 nm)	1032	206420	35.1% at 420 nm	[22]
	50 mg catalyst, 1.0 M $(NH_4)_2SO_3$		863	172600	29.3 % at 420 nm	
20 wt.% 1T MoS_2 NSs/CdS nanorods	10 mg catalyst, 10 % v/v lactic acid	500 W metal halide lamp (λ≥420 nm)	1324	132400	47.0% at 420 nm 4.0% at 460 nm	[23]
5 at.% MoS_2/CdS	80 mg catalyst, 10 % v/v lactic acid	300 W Xe lamp (λ≥420 nm)	20	250	3.7% at 420 nm	[24]
3 wt.% 1T- MoS_2 QDs/CdS	2 mg catalyst, 10 % v/v lactic acid	500 W metal halide lamp (λ≥420 nm)	263	131700	50.4% at 420 nm	[25]
70 wt.% MoS_2 NSs/ CdS nanowires	50 mg catalyst, 10 % v/v triethanolamine	300 W Xe lamp	90	1790	-	[26]
7 wt.% 2D/2D MoS_2/CdS	10 mg catalyst, 10 % v/v lactic acid	300 W Xe lamp (λ≥420 nm)	184	18430	3.5% at 450 nm	[27]
20 wt.% MoS_2 NSs/CdS NCAs	**20 mg catalyst, 0.35 M Na_2S, 0.25 M Na_2SO_3**	**300 W Xe lamp (λ≥420 nm)**	**390**	**19500**	**51.2% at 420 nm**	**This work**

Table S2. Fitting results of the EIS Nyquist data of pristine and MoS_2-modified CdS NCAs.

Sample	**R_s (Ω)**	**C_{dl} (F)**	**R_{ct} (kΩ)**	**Z_w (kΩ•$s^{-1/2}$)**	**x^2**
CdS NCAs	21.90	16.99×10^{-6}	13.5	61.9	3.8×10^{-5}
5-MoS_2/CdS	17.23	21.84×10^{-6}	6.3	3.6	4.6×10^{-4}
10-MoS_2/CdS	18.38	23.05×10^{-6}	5.6	3.6	5.3×10^{-4}
15-MoS_2/CdS	26.52	40.36×10^{-6}	5.3	1.7	3.1×10^{-5}
20-MoS_2/CdS	14.03	17.72×10^{-6}	2.7	3.5	9.7×10^{-4}
25-MoS_2/CdS	11.64	20.91×10^{-6}	4.5	3.1	5.5×10^{-4}
20-MoS_2/CdS_*b*	9.79	17.70×10^{-6}	5.2	4.5	6.8×10^{-4}

Table S3. PL lifetime biexponential decay model fitting parameters and calculated average lifetimes for the CdS, 20-MoS_2/CdS and 20-MoS_2/CdS_*b* NCAs.

Sample	**τ_1 (ns)**	**τ_2 (ns)**	**α_1 (%)**	**α_2 (%)**	**τ_{av}[a] (ns)**
CdS NCAs	0.35	3.97	77.6	22.4	3.12
20-MoS_2/CdS	0.51	4.85	64.8	35.2	4.15
20-MoS_2/CdS_*b*	0.49	4.09	63.8	36.2	3.46

[a]The average lifetime (τ_{av}) was calculated by the equation: $\tau_{av} = \left(\sum_i \alpha_i \tau_i^2\right) \Big/ \left(\sum_i \alpha_i \tau_i\right)$ (i = 1, 2).

Supporting Figures

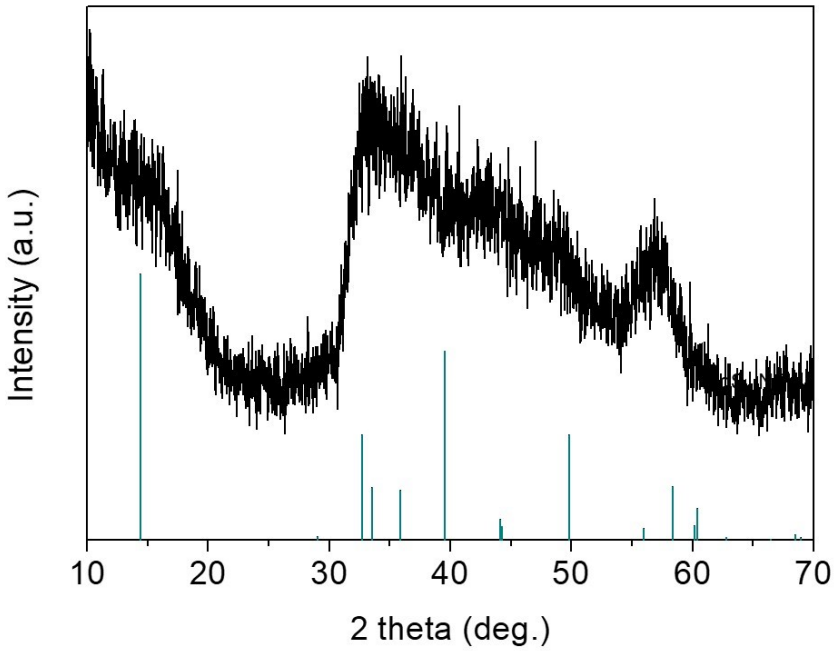

Fig. S1 XRD pattern of the MoS_2 NSs. The XRD pattern shows diffraction peaks that corresponds to the hexagonal (2H) phase of MoS_2 (JCPDS card no. 77-1716).

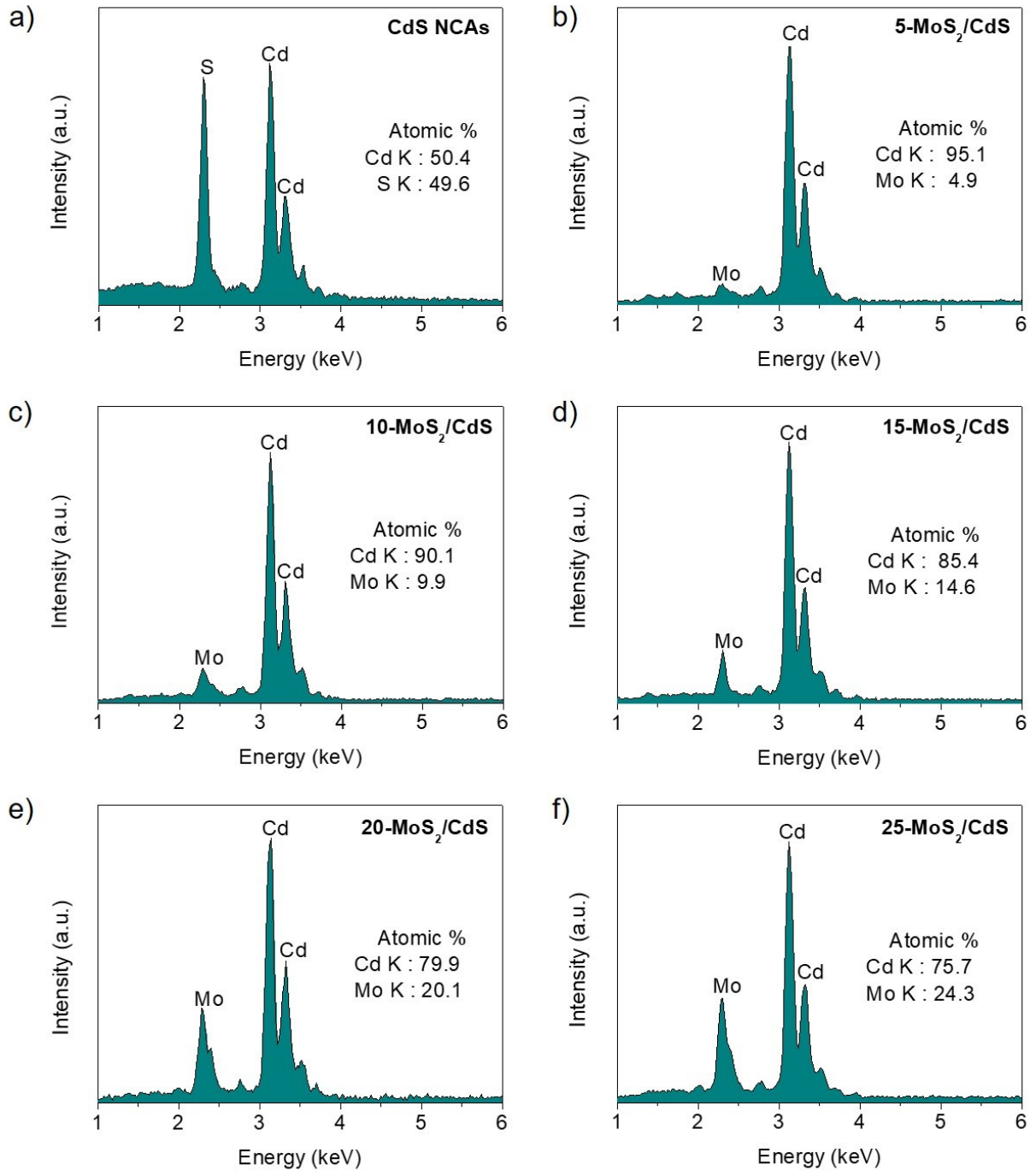

Fig. S2 Typical EDS spectra of the mesoporous CdS and *n*-MoS_2/CdS NCAs catalysts.

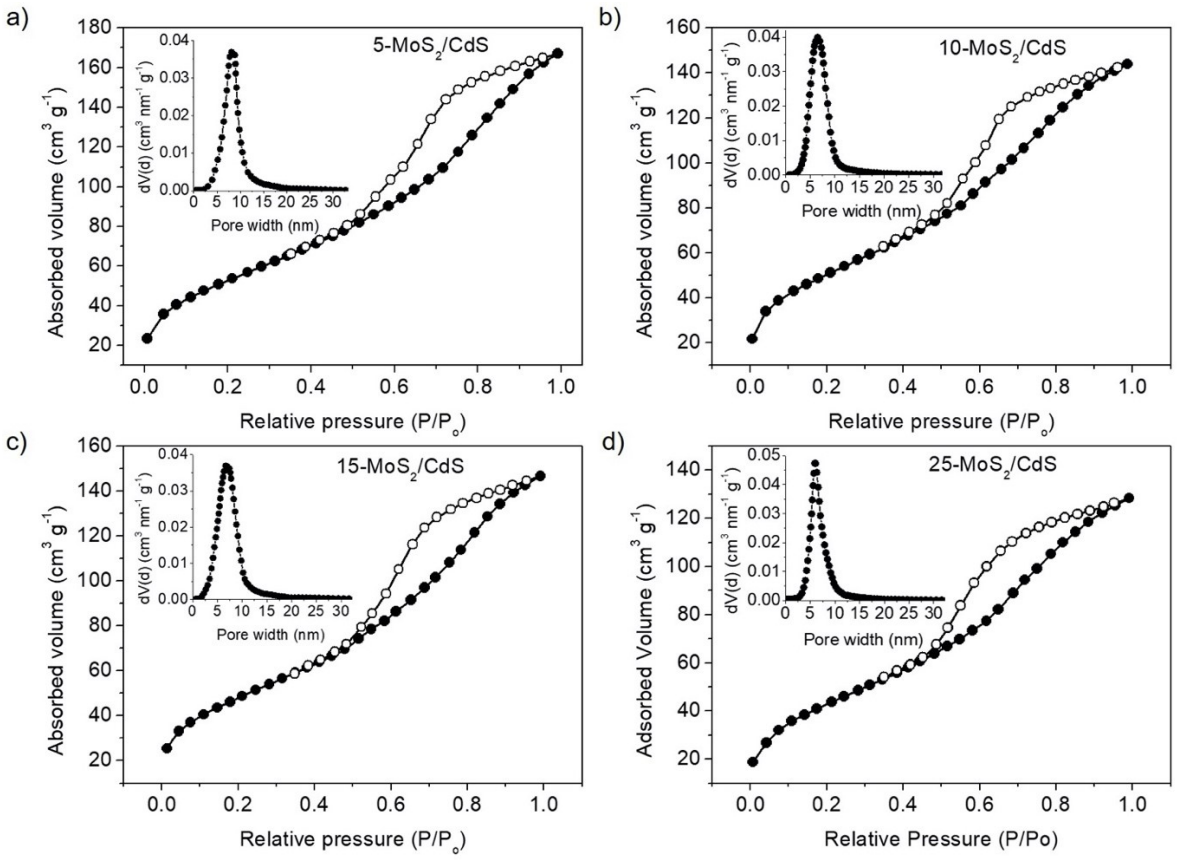

Fig. S3 N_2 adsorption (filled cycles) and desorption (open cycles) isotherms at –196 °C for the mesoporous (a) 5-MoS_2/CdS, (b)10-MoS_2/CdS, (c) 15-MoS_2/CdS and (d) 25-MoS_2/CdS NCAs. Insets: The corresponding NLDFT pore size distributions calculated from the adsorption branch of isotherms.

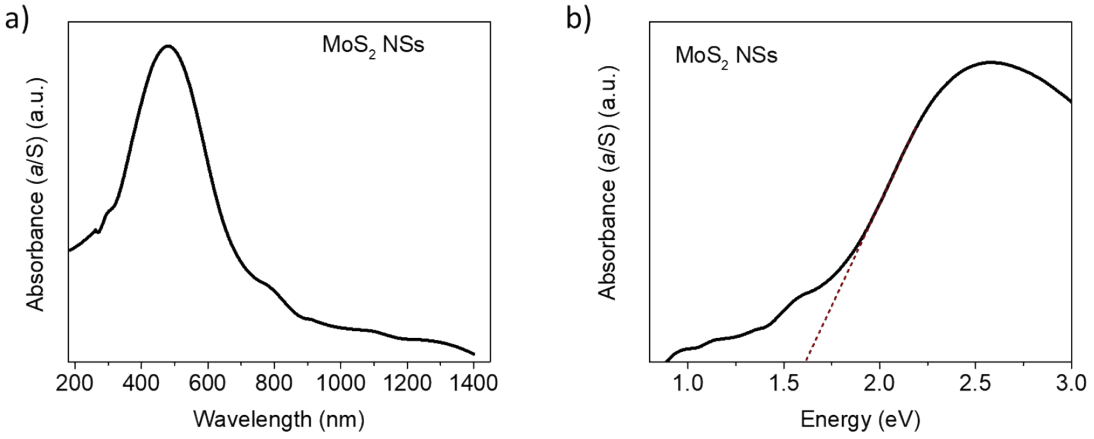

Fig. S4 (a) Optical absorption spectrum and (b) the corresponding absorbance vs energy plot of the as-synthesized MoS_2 NSs.

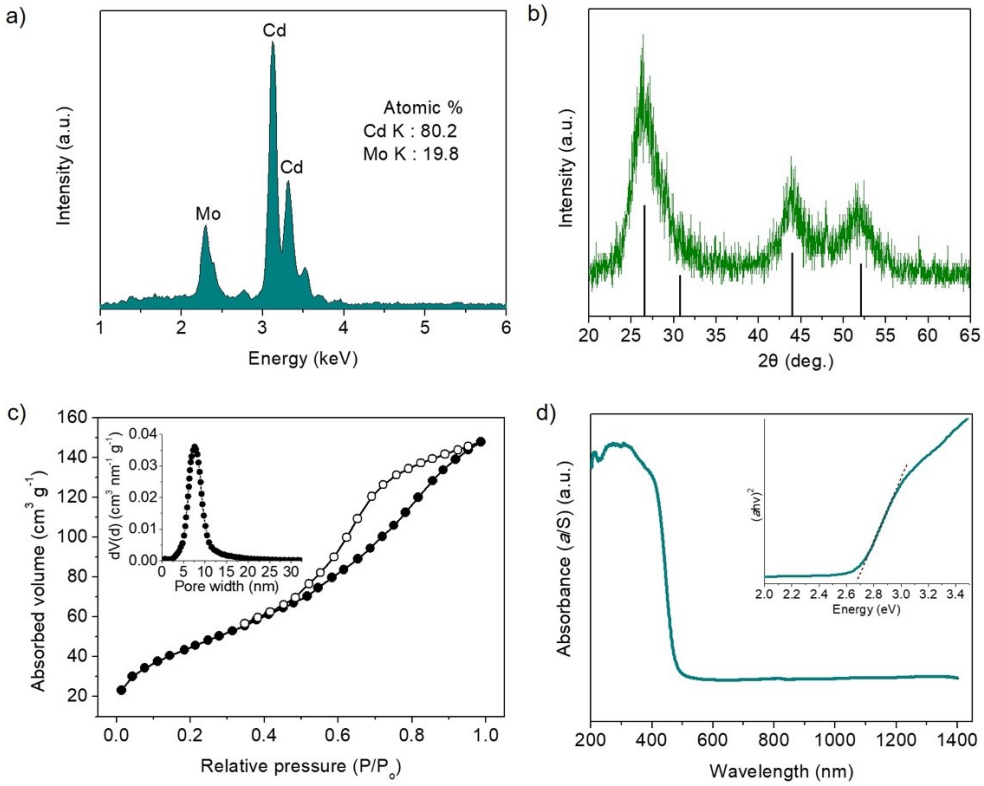

Fig. S5 (a) Typical EDS spectrum, (b) XRD pattern showing also the standard diffraction lines of zinc-blende CdS according to the JCPDS card No.42-1411, (c) Nitrogen adsorption-desorption isotherms at –196 °C and the corresponding NLDFT pore-size distribution plot (inset), and (d) optical absorption spectrum and Tauc plot (inset) of the mesoporous 20-MoS_2/CdS_*b* sample.

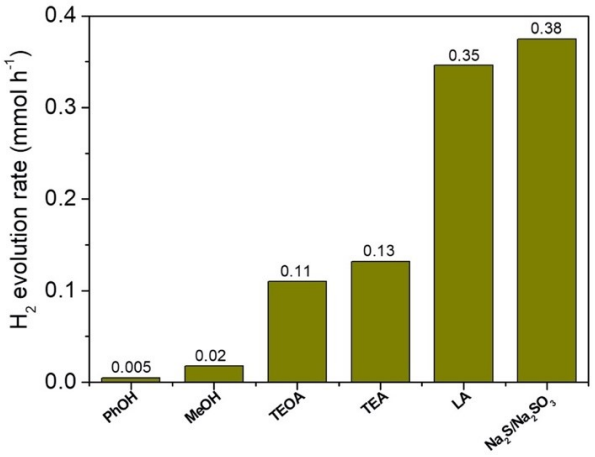

Fig. S6 Photocatalytic H_2 evolution rates for the mesoporous 20-MoS_2/CdS catalyst using different sacrificial reagents: phenol (PhOH, 0.35 M), methanol (MeOH, 10% v/v), triethanolamine (TEOA, 10% v/v), triethylamine (TEA, 10% v/v), lactic acid (LA, 10% v/v) and Na_2S/Na_2SO_3 (0.35 M/0.25 M) aqueous solution. All photocatalytic reactions were performed as follows: 20 mg of catalyst dispersed in a 20 mL aqueous solution containing the sacrificial reagent; 300 W Xe light radiation with a long-pass cut-off filter allowing λ ≥ 420 nm, 20 ±2 °C.

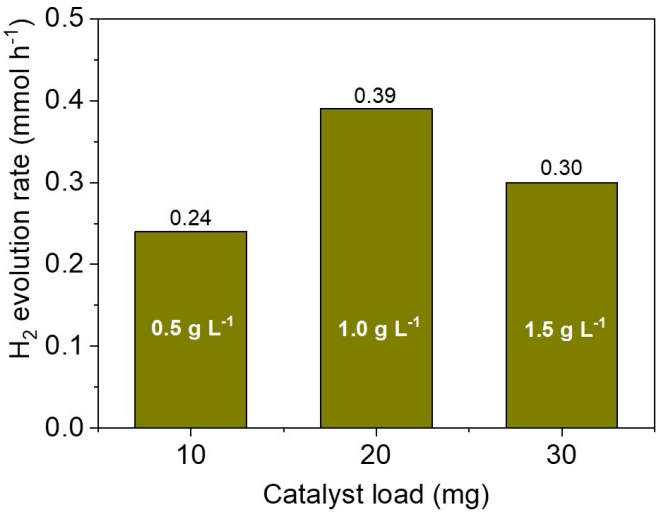

Fig. S7 Photocatalytic H_2 evolution activities for different loadings of 20-MoS_2/CdS catalyst. Experimental conditions: 10–30 mg of catalyst, 20 mL aqueous solution containing 0.35 M Na_2S and 0.25 M Na_2SO_3, 300 W Xenon light radiation with a long-pass cut-off filter (λ ≥ 420 nm), 20 ± 2 °C.

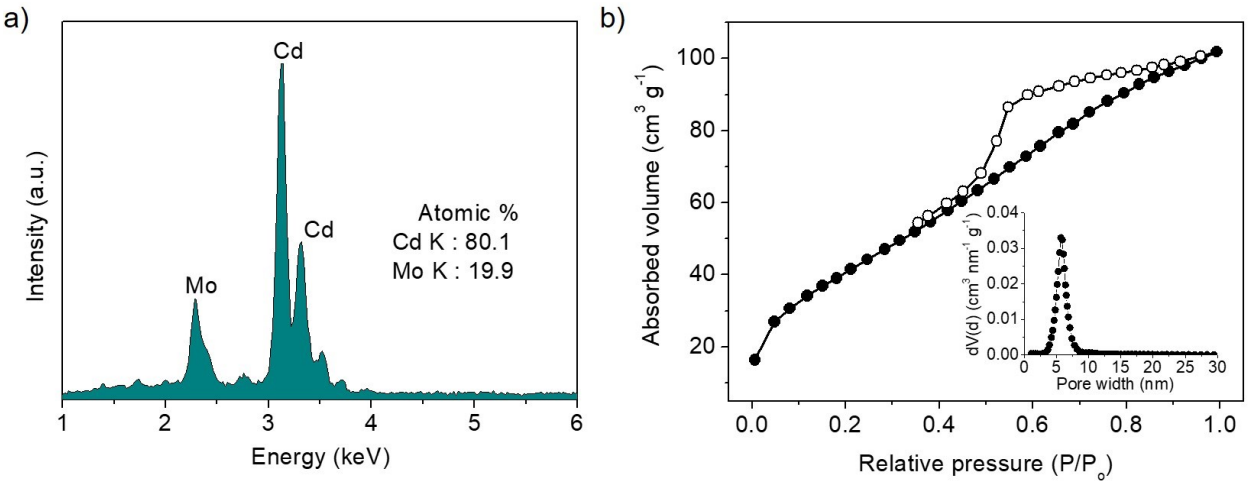

Fig. S8 (a) Typical EDS spectrum and (b) N_2 adsorption-desorption isotherms at – 196 °C and the corresponding NLDFT pore-size distribution (inset) for the 20-MoS_2/CdS catalyst retrieved after 15 h of photocatalytic reaction.

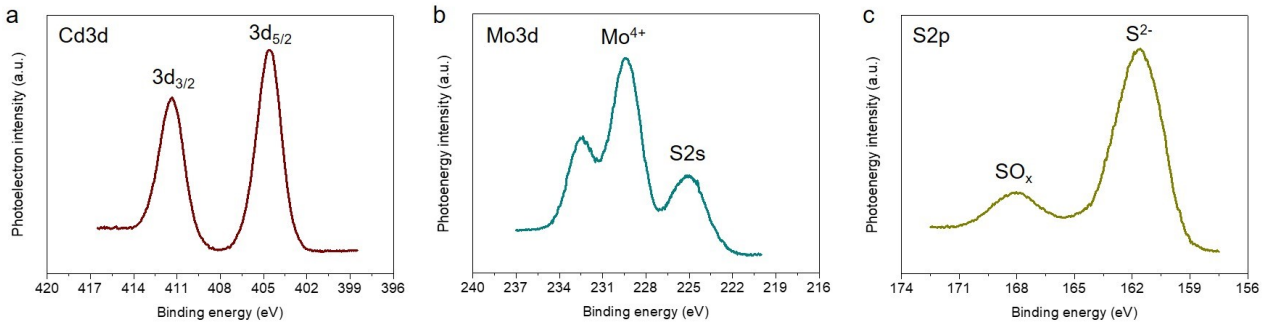

Fig. S9 Typical XPS core-level spectra of the (a) Cd 3d, (b) Mo 3d and (c) S 2p regions of the reused 20-MoS_2/CdS catalyst.

The Cd 3d XPS spectrum shows a doublet peak at 404.4 and 411.3 ± 0.2 eV, corresponding to the Cd $3d_{5/2}$ and Cd $3d_{3/2}$ core levels components of Cd^{2+} in CdS, respectively. The Mo 3d XPS spectrum shows two peaks at binding energies 229.3 and 232.5 ± 0.2 eV, which are assigned respectively to the $3d_{5/2}$ and $3d_{3/2}$ spin-orbit peaks of Mo^{4+} in MoS_2. The peak observed at 225.3 ± 0.2 eV is assigned to the S 2s line of sulfide (S^{2-}) ions. The S 2p XPS spectrum (**Fig. 2d**) shows a broad signal at 161.5 ± 0.3 eV due to the S^{2-} ions. In addition, a small amount of sulfur species at certain higher oxidation states is, however, observed in the surface of CdS and MoS_2 NSs, deducing from the weak peak at 168.1 ± 0.3 eV.

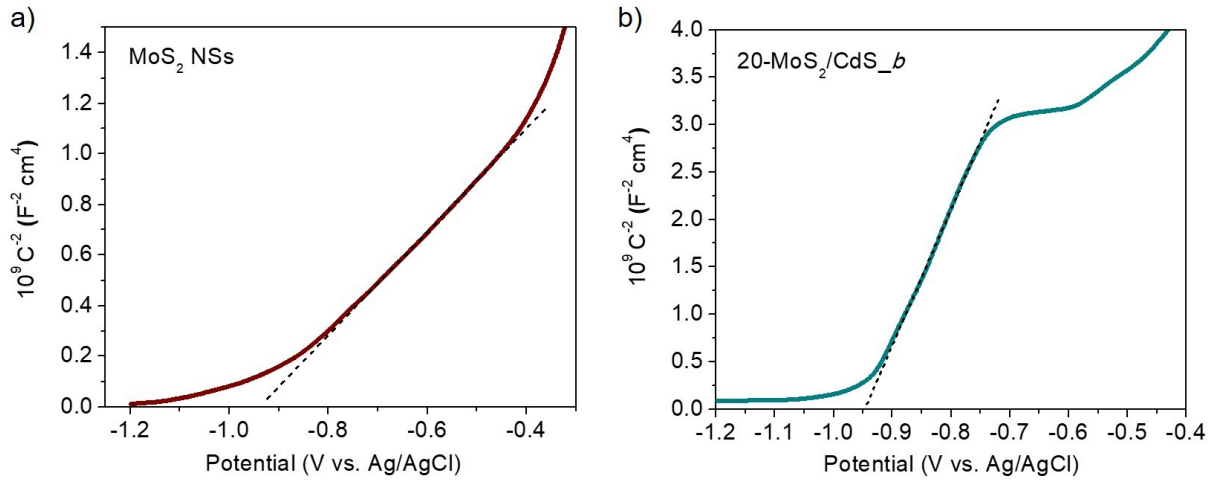

Fig. S10 Mott-Schottky plots of (a) as-prepared MoS_2 NSs and (b) mesoporous 20-MoS_2/CdS_*b* catalyst.

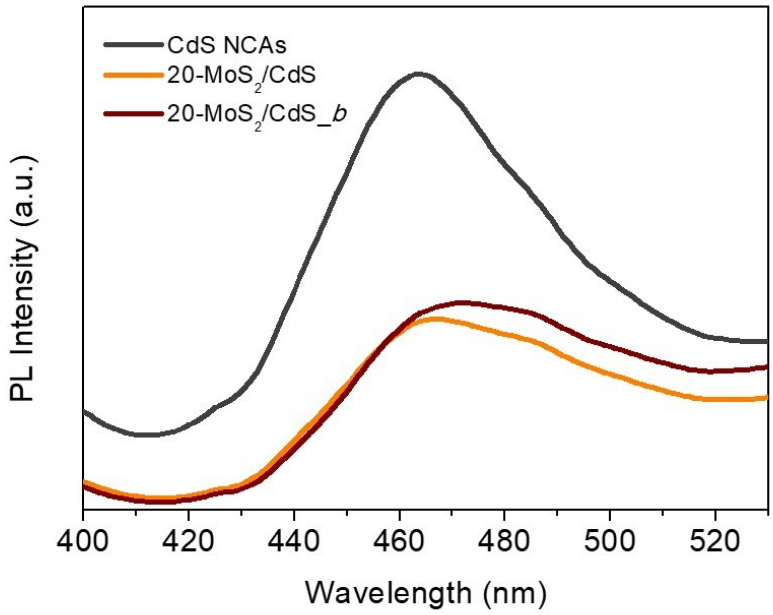

Fig. S11 Room-temperature PL spectra of pristine and MoS_2-modified CdS NCAs with 20 wt.% of MoS_2 NSs (20-MoS_2/CdS) and MoS_2 bulk flakes (20-MoS_2/CdS_*b*). PL emission spectra were obtained at a concentration of 0.5 mg mL^{-1} in water with an excitation wavelength of 375 nm.

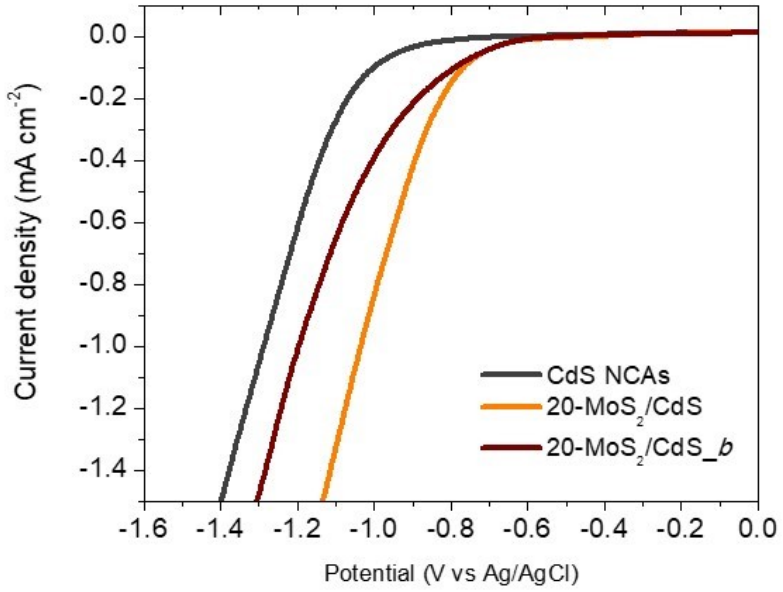

Fig. S12 J–V plots of CdS, 20-MoS_2/CdS and 20-MoS_2/CdS_*b* NCAs.

References

[1] X. Zong, G. Wu, H. Yan, G. Ma, J. Shi, F. Wen, L. Wang, C. Li, Photocatalytic H_2 Evolution on MoS_2/CdS Catalysts under Visible Light Irradiation, *J. Phys. Chem. C*, 2019, **114**, 1963–1968.

[2] X. Zong, H. Yan, G. Wu, G. Ma, F. Wen, L. Wang, C. Li, Enhancement of Photocatalytic H 2 Evolution on CdS by Loading MoS_2 as Cocatalyst under Visible Light Irradiation, *J. Am. Chem. Soc.*, 2008, **130**, 7176–7177.

[3] G. Chen, D. Li, F. Li, Y. Fan, H. Zhao, Y. Luo, R. Yu, Q. Meng Ball-milling combined calcination synthesis of MoS_2/CdS photocatalysts for high photocatalytic H_2 evolution activity under visible light irradiation, *Appl. Catal. A: Gen.*, 2012, **443**–**444**, 138–144.

[4] X.-Y. Liu, H. Yu, X. Quan, S. Chen, Green Synthesis of Feather-Shaped MoS_2/CdS Photocatalyst for Effective Hydrogen Production, *Int. J. Photoenergy*, 2013, 1–5.

[5] J. Zhang, Z. Zhu, X. Feng, Construction of Two-Dimensional MoS_2/CdS p-n Nanohybrids for Highly Efficient Photocatalytic Hydrogen Evolution, *Chem. Eur. J.*, 2014, **20**, 10632–10635.

[6] J. Xiong, Y. Liu, D. Wang, S. Liang, W. Wu, L. Wu, An efficient cocatalyst of defect-decorated MoS_2 ultrathin nanoplates for the promotion of photocatalytic hydrogen evolution over CdS nanocrystal, *J. Mater. Chem. A*, 2015, **3**, 12631–12635.

[7] K. Chang, M. Li, T. Wang, S. Ouyang, P. Li, L. Liu, J. Ye, Drastic Layer-Number-Dependent Activity Enhancement in Photocatalytic H_2 Evolution over nMoS_2/CdS (n ≥ 1) Under Visible Light, *Adv. Energy Mater.*, 2015, **5**, 1402279.

[8] J. Xu, X. Cao, Characterization and mechanism of MoS_2/CdS composite photocatalyst used for hydrogen production from water splitting under visible light, *Chem. Eng. J.*, 2015, **260**, 642–648.

[9] D. Lang, T. Shen, Q. Xiang, Roles of MoS_2 and Graphene as Cocatalysts in the Enhanced Visible-Light Photocatalytic H_2 Production Activity of Multiarmed CdS Nanorods, *ChemCatChem*, 2015, **7**, 943–951.

[10] F. Ma, Y. Wu, Y. Shao, Y. Zhong, J. Lv, X. Hao, 0D/2D nanocomposite visible light photocatalyst for highly stable and efficient hydrogen generation via recrystallization of CdS on MoS_2 nanosheets, *Nano Energy*, 2016, **27**, 466–474.

[11] J. He, L. Chen, F. Wang, Y. Liu, P. Chen, C.-T. Au, S.-F. Yin, CdS Nanowires Decorated with Ultrathin MoS_2 Nanosheets as an Efficient Photocatalyst for Hydrogen Evolution, *ChemSusChem*, 2016, **9**, 624–630.

[12] X. Zhou, J. Huang, H. Zhang, H. Sun, W. Tu, Controlled synthesis of CdS nanoparticles and their surface loading with MoS_2 for hydrogen evolution under visible light, *Int. J. Hydrog. Energy*, 2016, **41**, 14758–14767.

[13] X.-L. Yin, L.-L. Li, W.-J. Jiang, Y. Zhang, X. Zhang, L.-J. Wan, J.-S. Hu, MoS_2/CdS Nanosheets-on-Nanorod Heterostructure for Highly Efficient Photocatalytic H_2 Generation under Visible Light Irradiation, *ACS Appl. Mater. Interfaces*, 2016, **8**, 15258–15266.

[14] D. P. Kumar, S. Hong, D. A. Reddy, T. K. Kim, Noble metal-free ultrathin MoS_2 nanosheet-decorated CdS nanorods as an efficient photocatalyst for spectacular hydrogen evolution under solar light irradiation, *J. Mater. Chem. A*, 2016, **4**, 18551–18558.

[15] S. Ma, J. Xie, J. Wen, K. He, X. Li, W. Liu, X. Zhang, Constructing 2D layered hybrid CdS nanosheets/MoS_2 heterojunctions for enhanced visible-light photocatalytic H_2 generation, *Appl. Surf. Sci.*, 2017, **391**, 580–591.
[16] A. Wu, C. Tian, Y. Jiao, Q. Yan, G. Yang, H. Fu, Sequential two-step hydrothermal growth of MoS_2/CdS core-shell heterojunctions for efficient visible light-driven photocatalytic H_2 evolution, *Appl. Catal. B: Environ.*, 2017, **203**, 955–963.
[17] X. Hai, W. Zhou, S. Wang, H. Pang, K. Cheng, F. Ichihara, J. Ye, Rational design of freestanding MoS_2 monolayers for hydrogen evolution reaction, *Nano Energy*, 2017, **39**, 409–417.
[18] S. Zhang, H. Yang, H. Gao, R. Cao, J. Huang, X. Xu, One-pot synthesis of CdS irregular nanospheres hybridized with oxygen-incorporated defect-rich MoS_2 ultrathin nanosheets for efficient photocatalytic hydrogen evolution, *ACS Appl. Mater. Interfaces*, 2017, **9**, 23635–23646.
[19] L. Zhao, J. Jia, Z. Yang, J. Yu, A. Wang, Y. Sang, W. Zhou, H. Liu, One-step synthesis of CdS nanoparticles/MoS_2 nanosheets heterostructure on porous molybdenum sheet for enhanced photocatalytic H_2 evolution, *Appl. Catal. B: Environ.*, 2017, **210**, 290–296.
[20] B. Chai, M. Xu, J. Yan, Z. Ren, Remarkably enhanced photocatalytic hydrogen evolution over MoS_2 nanosheets loaded on uniform CdS nanospheres, *Appl. Surf. Sci.*, 2018, **430**, 523–530.
[21] L. Jiang, L. Wang, G. Xu, L. Gu, Y. Yuan, A microwave-assisted thermolysis route to single-step preparation of MoS_2/CdS composite photocatalysts for active hydrogen generation, *Sustain. Energy Fuels*, 2018, **2**, 430–435.
[22] J. Sun, L. Duan, Q. Wu, W. Yao, Synthesis of MoS_2 quantum dots cocatalysts and their efficient photocatalytic performance for hydrogen evolution, *Chem. Eng. J.*, 2018, **332**, 449–455.
[23] X.-H. Zhang, N. Li, J. Wu, Y.-Z. Zheng, X. Tao, Defect-rich O-incorporated 1T-MoS_2 nanosheets for remarkably enhanced visible-light photocatalytic H_2 evolution over CdS: The impact of enriched defects, *Appl. Catal. B: Environ.*, 2018, **229**, 227–236.
[24] Z.-W. Zhang, Q.-H. Li, X.-Q. Qiao, D. Hou, D.-S. Li, One-pot hydrothermal synthesis of willow branch-shaped MoS_2/CdS heterojunctions for photocatalytic H_2 production under visible light irradiation, *Chin. J. Catal.*, 2019, **40**, 371–379.
[25] X. Li, X. Lv, N. Li, J. Wu, Y.-Z. Zheng, X. Tao, One-step hydrothermal synthesis of high-percentage 1T-phase MoS_2 quantum dots for remarkably enhanced visible-light-driven photocatalytic H_2 evolution, *Appl. Catal. B: Environ.*, 2019, **243**, 76–85.
[26] W. Zhao, J. Liu, Z. Ding, J. Zhang, X. Wang, Optimal synthesis of platinum-free 1D/2D CdS/MoS_2 (CM) heterojunctions with improved photocatalytic hydrogen production performance, J. Alloys Compd., 2020, **813**, 152234.
[27] M. Xiong, J. Yan, B. Chai, G. Fan, G. Song, Liquid exfoliating CdS and MoS_2 to construct 2D/2D MoS_2/CdS heterojunctions with significantly boosted photocatalytic H_2 evolution activity, *J. Mater. Sci. Technol.*, 2020, **56**, 179–188.